WISCONSIN ELECTRIC POWER COMPANY
POINT BEACH NUCLEAR PLANT
UNIT 2 CYCLE 11 STARTUP
JANUARY, 1985

BY
R. L. HARRIS
P. N. KURTZ

TABLE OF CONTENTS

LIST OF TABLES

LIST OF FIGURES

PREFACE

This report is intended to document in a concise format the results of the physics testing program and unit systems response during the startup of Unit 2 following Refueling 10. The organization of the report follows that utilized previously in startup reports.

The core loading pattern was determined by Westinghouse, the vendor for the nuclear steam supply system. WCAP 10583, Revision 1 "The Nuclear Design - Core Management of the Point Beach Unit 2 Nuclear Reactor Cycle 11," tabulates various parameters predicted by computer codes. All references in this report to design values pertain to WCAP 10583. Actual end of Cycle 10 burnup was 13,677 MWD/MTU. The published WCAP parameters were based on actual Cycle 10 EOL burnup. Cycle 10 was ended on September 28, 1984 with a peak assembly burnup of 42,730 MWD/MTU and average assembly burnup of 24,108 MWD/MTU. Electrical power was first generated during Cycle 11 on November 20, 1984.

This report is intended primarily for the use of Wisconsin Electric Power Company personnel as a readily accessible, complete compilation of reduced data.

Copies of this report were submitted to the NRC to comply with Technical Specification 15.6.9.1.A.1.c and 15.6.9.1.A.2. A region of Westinghouse optimized fuel assemblies (OFA's) was loaded for the first time at PBNP in Unit 2 Cycle 11. The fuel design changes for OFA's were significant enough to be classified as constituting a different fuel design.

Section 1.0 REFUELING

Section 1.1 Core Unload

The core was completely unloaded to facilitate incore thimble changeout and reactor vessel component inspections. The first fuel assembly was unloaded on October 13, 1984 at 1842 hours. Using two 10-hour shifts per day, the unload was completed without any changes to the sequence on October 15, 1984, at 1752 hours.

All fuel was stored in the north spent fuel pit. Spent fuel receipt was suspended between core unload and core reload with one spent fuel assembly (D14) not put in the spent fuel pit.

There were no insert changes made during core unload.

One fuel assembly (M55) sustained grid damage when being placed in storage location SM-27. It was replaced with fuel assembly N02 for the core reload.

Section 1.2 Insert Changes

1. Eight RCCA's were replaced because of wear found during visual inspections performed in 1983. All control rod transfers were made without incident.

2. Several depleted burnable poison (BP) assemblies were removed from o transferred between reload fuel assemblies with no incident.

3. Three new BP assemblies were transferred between new fuel assemblies. A fourth BP assembly could not be transferred because it repeatedly fell from the tool's gripper mechanism when lifted from a new fuel assembly. One of the new BP assemblies that were successfully transferred was then partially withdrawn by the tool in front of the periscope. It was discovered that the BP assembly crossbar was wedged in the gripper mechanism below the latching fingers. Apparently the three transfers were made with the BP assemblies held in the tool by friction.

   The fourth BP assembly was transferred to the new fuel vault so that it could be inspected at a later date. It was replaced with a new BP assembly left over from Unit 1.

4. One plug device was damaged when a top nozzle spring clamp with orientation hole broke off and wedged between the plug device tool and top nozzle of fuel assembly K77. Several spare plug devices were available for replacement because of the changeover to optimized fuel requiring new redesigned plug devices. A spare plug device was put in fuel assembly K68 (replacement for K77).

All other plug device changes were made without incident.

Section 1.3 Fuel Assembly Inspections

OFA demonstration assemblies ZD1, ZD2, and ZD4 were inspected by Westinghouse. These assemblies have removable rods and have had 3 cycles of burnup. The inspection program included general visual examinations of the fuel assemblies and high magnification visual examination of several individual fuel rods. No abnormalities were found.

Section 1.4 Core Reload

Changes were made to the original core loading plan for Cycle 10 because of damage to the following fuel assemblies:

1. M55 - Replaced with N02 after sustaining grid damage from spent fuel pit storage rack at location SM-27.

2. K77 - Replaced with K68 after the top nozzle spring clamp with orientation hole broke off.

As a result of the above replacements, changes were made to the original core loading sequence as described in Table 1-1.

Numerous changes had to be made to the core loading sequence because assemblies were bowed. This problem is expected to occur during full core reloads.

TABLE 1-1

CHANGES TO CORE LOADING PLAN

	Original		Final	
Core Location	F/A	Insert	F/A	Insert
E-3	M55	RCCA	M77	RCCA
D-4	M77	RCCA	N02	RCCA
G-1	ZD2	ZPD	K68	PD
G-13	K77	8P50	ZD2	ZPD
D-3	N81	2P105Z	N81	PDZ

Section 1.5 Core Design

1. Optimized Fuel Assemblies

A region of 32 new optimized fuel assemblies were used for the first time at PBNP in Cycle 11. Their distribution in core is typical of the low leakage concept in which new fuel assemblies are loaded between the center area and extreme periphery of the core.

Three demonstration optimized fuel assemblies with removable fuel rods were loaded for a fourth cycle of operation at peripheral locations A-7, G-13, and M-7. These assemblies were found to be in good condition when inspected prior to core load.

The optimized fuel assembly employs a slightly reduced fuel rod clad OD (0.400 inch) compared to the standard fuel rod clad OD (0.422 inch) while retaining the same fuel rod pitch. This increases the water to uranium ratio which improves neutron moderation and efficiency eventually lowering fuel cycle costs. The fuel pellets are enriched to 3.4% in U-235.

Another feature of the optimized fuel assembly design is the use of zircaloy spacer grids for all but the top and bottom spacer grids. The top and bottom spacer grids are Inconel, the same material used in standard fuel assembly spacer grids.

Slight reductions in the guide thimble and instrument thimble diameters were also made. Standard control rods and burnable poison rods are compatible with optimized fuel assemblies. Standard plug devices, all having thicker plugging rods are not compatible however, and new plug devices were provided for use in optimized fuel assemblies.

2. Inserts

New burnable poison assemblies were provided in Cycle 11 to control radial power distribution. Seven 2P and eight 14P asymmetric burnable poison assemblies were loaded in optimized fuel assemblies. Four 4P burnable poison assemblies were loaded in once-burned fuel near the core's center.

Eight control rods were replaced in a continuing program leading eventually to total replacement. A total of 10 original control rods have been replaced since the program started in 1983.

The two secondary sources were returned to their normal locations at G-2 and G-12.

3. Fuel Loading

Table 1-2 lists the uranium weight by region. Figure 1-1 shows the final core load pattern, Figure 1-2 BOL SNM data, and Figure 1-3 BOL burnup data.

TABLE 1-2

URANIUM LOADING

Region	Number of Assemblies	U Weight (MTU) Original	U Weight (MTU) Current	Current Enrichment (%U235)
9A	1	0.40	0.38	0.74
10	5	2.00	1.92	1.10
10A	3	1.06	1.01	0.75
11	28	11.24	10.86	1.23
13A	4	1.60	1.55	1.36
13B	1	0.40	0.39	1.65
12	7	2.81	2.76	2.05
12A	40	16.13	15.80	1.88
13*	32	11.40	11.40	3.40
	TOTAL	47.04	46.07	2.02

* New Assemblies

FIGURE 1-1

CORE LOADING

```
PBNP SNM DATA - UNIT 2 CYCLE 11  -  START OF CYCLE AS OF 10/26/84              11/14/84


     1      2      3      4      5      6      7      8      9      10     11     12     13


                                       L60    ZD1    L62
A                                      LM0AFQ LM03PK LM0AFL
                                       PD     SPD    PD

                         L52    N53    N60    M65    N63    N73    L77
B                        LM0AFY LM0E3S LM0E3K LM0BVD LM0E2X LM0E38 LM0AFC
                         PD     OPD    R   64 PD     R   84 OPD    PD

                  L72    N74    M52    N07    L63    L58    M58    N52    L55
C                 LM0AFG LM0E37 LM0AV9 LM09YD LM0AFN LM0AFT LM0AVQ LM0E3T LM0AFW
                  PD     2P 107 R   56 PD     R  114 PD     R   65 2P 100 PD

           L66    N81    N02    M79    N55    K59    N68    M97    M82    N69    L67
D          LM0AFM LM0E38 LM09YJ LM0BVE LM0E3Q LM03NU LM0E31 LM0BUG LM0BUX LM0E33 LM0AFK
           PD     OPD    R   76 PD     14P102 PD     14P100 PD     R   74 2P 102 PD

           N65    M77    M85    M64    M92    M88    M91    M81    M87    M57    N66
E          LM0E32 LM0BVA LM0BUR LM0BVF LM0BUU LM0BUM LM0BUW LM0BUZ LM0BUN LM0AVF LM0E34
           OPD    R   83 PD     R   57 PD     PD     PD     R   68 PD     R   72 OPD

    L59    N59    L54    N62    M67    M76    M89    M68    M63    N51    N08    N72    L61
F   LM0AFS LM0E3L LM0AFX LM0E3H LM0BV9 LM0BV8 LM0BUF LM0BV7 LM0BVH LM0E3U LM09YC LM0E35 LM0AFJ
    PD     R   55 PD     14P105 PD     R   80 4P 102 R   69 PD     14P104 PD     R  107 PD

    K68    M61    L73    K51    M80    M70    J76    M98    M90    K61    L71    M95    ZD2
G   LM03PE LM0BVK LM0AFF LM03PQ LM0BVG LM0BV3 LM07U7 LM0BUE LM0BUY LM03P9 LM0AFH LM0BUM LM03PL
    PD     SPS  3 R  115 PD     PD     4P 100 R   77 4P 101 PD     PD     R  112 SPS  4 SPD

    L51    N58    N05    N57    M66    M69    M96    M83    M94    N79    L53    N77    L70
H   LM0AG0 LM0E3M LM09YF LM0E3P LM0BVB LM0BV5 LM0BUK LM0BUV LM0BUQ LM0E3E LM0AFZ LM0E3C LM0AF9
    PD     R   61 PD     14P103 PD     R   79 4P 103 R   63 PD     14P107 PD     R  110 PD

           N71    M56    M86    M74    M59    M75    M60    M73    M84    M51    N82
I          LM0E2Y LM0AVE LM0BUL LM0BV4 LM0BUJ LM0BV6 LM0BUP LM0BV2 LM0BUT LM0AVA LM0E3F
           OPD    R   75 PD     R   62 PD     PD     PD     R   81 PD     R   66 OPD

           L75    N70    M93    M62    N67    K70    N76    M71    M78    N56    L74
J          LM0AFD LM0E36 LM0BUS LM0BVJ LM0E27 LM03PC LM0E39 LM0BV1 LM0BVC LM0E3N LM0AFE
           PD     2P 103 R   73 PD     14P106 PD     14P101 PD     R   82 2P 104 PD

                  L69    N80    M54    L64    L57    N06    M53    N54    L65
K                 LM0AF8 LM0E3D LM0AVC LM0AFR LM0AFU LM09YE LM0AVB LM0E3R LM0AFP
                  PD     2P 101 R   54 PD     R  116 PD     R   34 2P 106 PD

                         L78    N61    N75    M72    N64    N78    L68
L                        LM0AFA LM0E3J LM0E3A LM0BV0 LM0E30 LM0E3B LM0AF7
                         PD     OPD    R  111 PD     R  109 OPD    PD

                                       L56    ZD4    L76
M                                      LM0AFV LM03PN LM0AFB
                                       PD     SPD    PD
```

FIGURE 1-2

BOL SNM DATA

PBNP SNM DATA - UNIT 2 CYCLE 11 - START OF CYCLE AS OF 10/26/84 11/14/84

	1	2	3	4	5	6	7	8	9	10	11	12	13
A						L60 4564 2434	Z01 2509 2020	L62 4517 2444					
B				L52 4574 2447	N53 12216 0	N60 12021 0	M65 9227 1414	N63 12230 0	N73 12139 0	L77 4528 2448			
C			L72 4987 2371	N74 12038 0	M52 8084 1744	N07 5261 2232	L63 4846 2385	L58 5255 2351	M58 8126 1726	N52 12066 0	L55 4981 2375		
D		L66 4600 2442	N81 12116 0	M02 6446 2019	M79 7290 1949	N55 12040 0	K59 4543 2493	N68 12081 0	M97 7346 1959	M82 7326 1941	N69 11998 0	L67 4527 2434	
E		N65 11983 0	M77 7402 1923	M85 7335 1954	M64 6737 2078	M92 6690 2095	M88 7337 1938	M91 6743 2086	M81 6713 2083	M87 7254 1951	M57 8070 1720	N66 12055 0	
F	L59 4556 2439	N59 12034 0	L54 5185 2353	N62 12028 0	M67 6665 2097	M76 6758 2070	M89 8967 1521	M68 6779 2073	M63 6665 2087	N51 12028 0	N08 5318 2240	N72 12039 0	L61 4605 2437
G	K68 3121 2644	M61 9297 1414	L73 4872 2396	K51 4506 2492	M80 7419 1934	M70 8034 1538	J76 2818 2674	M98 8883 1543	M90 7341 1940	K61 4509 2503	L71 4828 2391	M95 9184 1421	Z02 2558 2018
H	L51 4563 2441	N58 12006 0	N05 5253 2846	N57 12088 0	M66 6723 2088	M04 6703 2081	M96 8936 1531	M83 6799 2080	M94 6687 2087	N79 12035 0	L53 5156 2343	N77 12132 0	L70 4610 2440
I		N71 12045 0	M56 8125 1729	M86 7213 1970	M74 6732 2071	M59 6673 2102	M75 7336 1940	M60 6712 2090	M73 6649 2088	M84 7221 1959	M51 8039 1743	N82 12002 0	
J		L75 4582 2428	N70 12029 0	M93 7346 1943	M62 7365 1957	N67 12089 0	K70 4492 2504	N76 12020 0	M71 7259 1954	M78 7481 1925	N56 12026 0	L74 4620 2441	
K			L69 5084 2376	N80 12069 0	M54 8012 1758	L64 5198 2337	L57 5023 2394	N06 5245 2249	M53 8114 1733	N54 12024 0	L65 5040 2363		
L				L78 4526 2432	N61 12196 0	N75 11987 0	M72 9238 1429	N64 12036 0	N78 12027 0	L68 4567 2431			
M						L56 4603 2459	Z04 2570 2017	L76 4564 2427					

CONTENTS OF EACH CORE LOCATION

FUEL IDENTIFICATION #
CURRENT U-235 GRAMS
CURRENT FISSILE PU GRAMS

FIGURE 1-3

BOL BURNUP DATA

PBNP UNIT 2 CYCLE 11 - START OF CYCLE BURNUP DATA - 11/14/84

	1	2	3	4	5	6	7	8	9	10	11	12	13
A						L60 15452 26268	ZD1 16770 36823	L62 15633 26545					
B				L52 15644 26246	N53 0 0	N60 0 0	M65 8895 8895	N63 0 0	M73 0 0	L77 15586 26499			
C			L72 16915 24093	N74 0 0	M52 12276 12276	N07 15849 22635	L63 16140 24729	L58 14382 23006	M58 12131 12131	N52 0 0	L55 16891 24186		
D		L66 15673 26122	N81 0 0	N02 8968 17592	M79 14937 14937	N55 0 0	K59 6374 28146	N68 0 0	M97 14954 14954	M82 14866 14866	N69 0 0	L67 15693 26360	
E		N65 0 0	M77 14564 14564	M85 14937 14937	M64 16960 16960	M92 17254 17254	M88 14764 14764	M91 16984 16984	M81 17036 17036	M87 15065 15065	M57 12094 12094	N66 0 0	
F	L59 15624 26301	N59 0 0	L54 14615 23290	N62 0 0	M67 17283 17283	M76 16877 16877	M89 9787 9787	M68 16833 16833	M63 17242 17242	N51 0 0	N08 15776 22522	N72 0 0	L61 15600 26078
G	K68 14847 36943	M61 8806 8806	L73 15983 24711	K51 6419 28263	M80 14597 14597	M70 10026 10026	J76 5099 39130	M98 10014 10014	M90 14774 14774	K61 6533 28350	L71 15917 24849	M95 8943 8943	ZD2 16201 36428
H	L51 15551 26309	N58 0 0	N05 15865 22765	N57 0 0	M66 17075 17075	M69 17224 17224	M96 9886 9886	M83 16898 16898	M94 17163 17163	N79 0 0	L53 14479 23316	N77 0 0	L70 15736 26145
I		N71 0 0	M56 12171 12171	M86 15232 15232	M74 17069 17069	M59 17290 17290	M75 14801 14801	M60 17139 17139	M73 17421 17421	M84 15124 15124	M51 12414 12414	M82 0 0	
J		L75 15738 26119	N70 0 0	M93 14846 14846	M62 14918 14918	N67 0 0	K70 6552 28435	N76 0 0	M71 15137 15137	M78 14476 14476	N56 0 0	L74 15695 26075	
K			L69 16854 23802	N80 0 0	M54 12513 12513	L64 14358 23106	L57 15613 24168	N06 15811 22805	M53 12194 12194	N54 0 0	L65 16848 23871		
L				L78 15865 26387	N61 0 0	M75 0 0	M72 8955 8955	N64 0 0	M78 0 0	L68 15689 26200			
M						L56 15652 26307	ZD4 16624 36416	L76 15474 26206					

CONTENTS OF EACH CORE LOCATION

FUEL IDENTIFICATION #
CYCLE ASSEMBLY BURNUP
TOTAL ASSEMBLY BURNUP

PBNP UNIT 2 CYCLE 11 - START OF CYCLE BURNUP DATA - 11/14/84

Section 2.0 CONTROL ROD OPERATIONAL TESTING

Cold control rod testing was conducted on November 15, 1984, just prior to initial cycle heatup.

Hot control rod testing was conducted shortly after primary system heatup on November 17, 1984.

Section 2.1 Rod Drop Times

Rod drop times to dashpot in the cold full-flow condition ranged from 1.27 seconds to 1.50 seconds with several rod drop times near each end of the range.

Rod drop times to dashpot in the hot zero flow condition ranged from 1.08 seconds to 1.18 seconds with several rod drop times near each end of the range.

Rod drop times to dashpot in the hot full-flow condition ranged from 1.23 seconds to 1.36 seconds with several rod drop times near each end of the range.

See Figures 2-1 through 2-3 for rod drop times and core parameters. Locations containing optimized fuel assemblies are marked because the narrower thimble tubes increase rod drop times slightly in the dashpot area. Locations with new control rods are also shown.

All rod drop times to dashpot were well within the Technical Specification limit of 2.2 seconds (15.3.10.E).

Section 2.2 Control Rod Mechanism Timing

Control rod mechanism timing was conducted in cold plant conditions on November 15, 1984. The visicorder traces of the lift, movable and stationary gripper coil voltages of each rod mechanism were reviewed by plant personnel. No rod misstepping occurred.

Section 2.3 Rod Position Calibration

During hot rod testing, LVDT voltages were read at 20 steps and 200 steps to determine if any voltages were abnormal.

"Zero" adjustments were made with rods at 20 steps under hot zero power full flow conditions.

"Span" adjustments were made at full power after rods were verified to be at 228 steps using WMTP 9.19.

FIGURE 2-1

COLD ROD DROP TIMES (FULL FLOW)

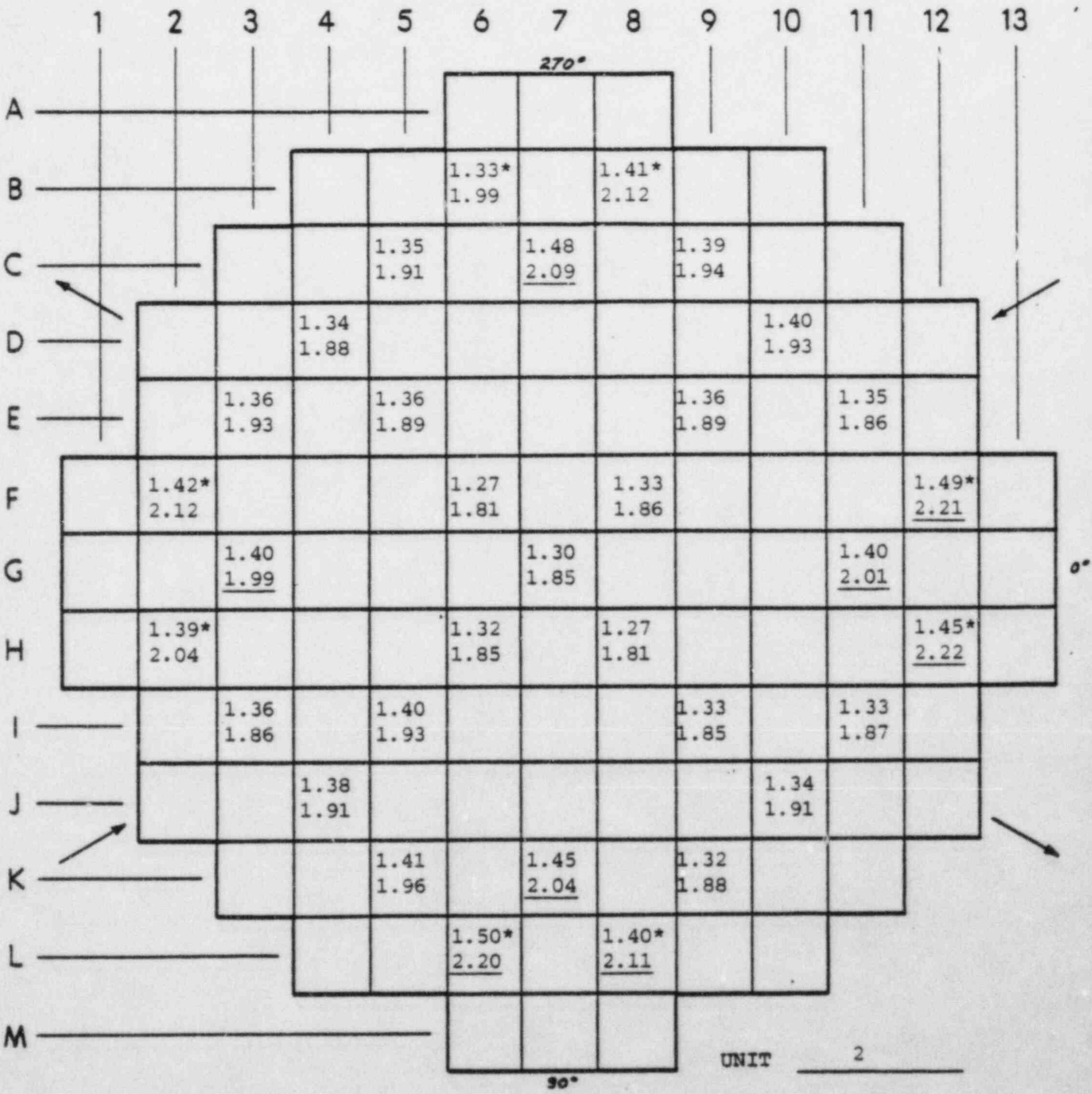

	1	2	3	4	5	6	7	8	9	10	11	12	13
A													
B						1.33* 1.99		1.41* 2.12					
C					1.35 1.91		1.48 2.09		1.39 1.94				
D				1.34 1.88						1.40 1.93			
E			1.36 1.93		1.36 1.89				1.36 1.89		1.35 1.86		
F		1.42* 2.12				1.27 1.81		1.33 1.86				1.49* 2.21	
G			1.40 1.99				1.30 1.85				1.40 2.01		
H		1.39* 2.04				1.32 1.85		1.27 1.81				1.45* 2.22	
I			1.36 1.86		1.40 1.93				1.33 1.85		1.33 1.87		
J				1.38 1.91						1.34 1.91			
K					1.41 1.96		1.45 2.04		1.32 1.88				
L						1.50* 2.20		1.40* 2.11					
M													

* ← Optimized Fuel Assembly
← TIME TO DASHPOT (SEC)
← TIME TO BOTTOM (SEC)
____ ← New Control Rod

UNIT 2
DATE 11-15-84
TEMP. 295 °F
FLOW 100 %
PRESSURE 340 psia

POINT BEACH NUCLEAR PLANT

CONTROL ROD TESTING
ROD DROP TIMES

FIGURE 2-2

HOT ROD DROP TIMES (NO FLOW)

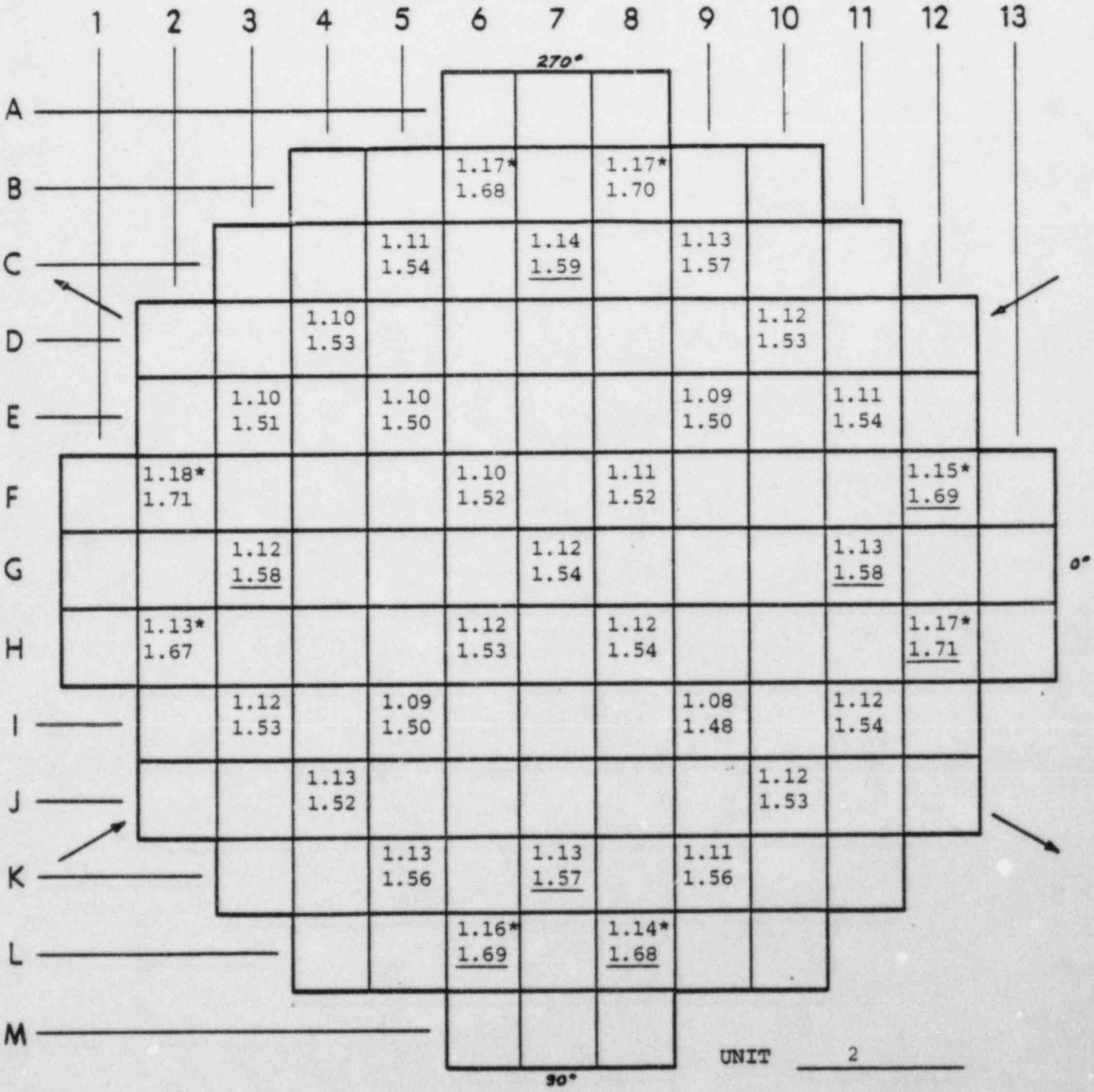

	1	2	3	4	5	6	7	8	9	10	11	12	13
A													
B						1.17* 1.68		1.17* 1.70					
C					1.11 1.54		1.14 1.59		1.13 1.57				
D				1.10 1.53						1.12 1.53			
E			1.10 1.51		1.10 1.50				1.09 1.50		1.11 1.54		
F		1.18* 1.71				1.10 1.52		1.11 1.52				1.15* 1.69	
G			1.12 1.58				1.12 1.54				1.13 1.58		
H		1.13* 1.67				1.12 1.53		1.12 1.54				1.17* 1.71	
I			1.12 1.53		1.09 1.50				1.08 1.48		1.12 1.54		
J				1.13 1.52						1.12 1.53			
K					1.13 1.56		1.13 1.57		1.11 1.56				
L						1.16* 1.69		1.14* 1.68					
M													

* ← Optimized Fuel Assembly
← TIME TO DASHPOT (SEC)
← TIME TO BOTTOM (SEC)
____ ← New Control Rod

UNIT 2
DATE 11-17-84
TEMP. ~520 °F
FLOW 0 %
PRESSURE ~1990 psia

POINT BEACH NUCLEAR PLANT

CONTROL ROD TESTING
ROD DROP TIMES

FIGURE 2-3

HOT ROD DROP TIMES (FULL FLOW)

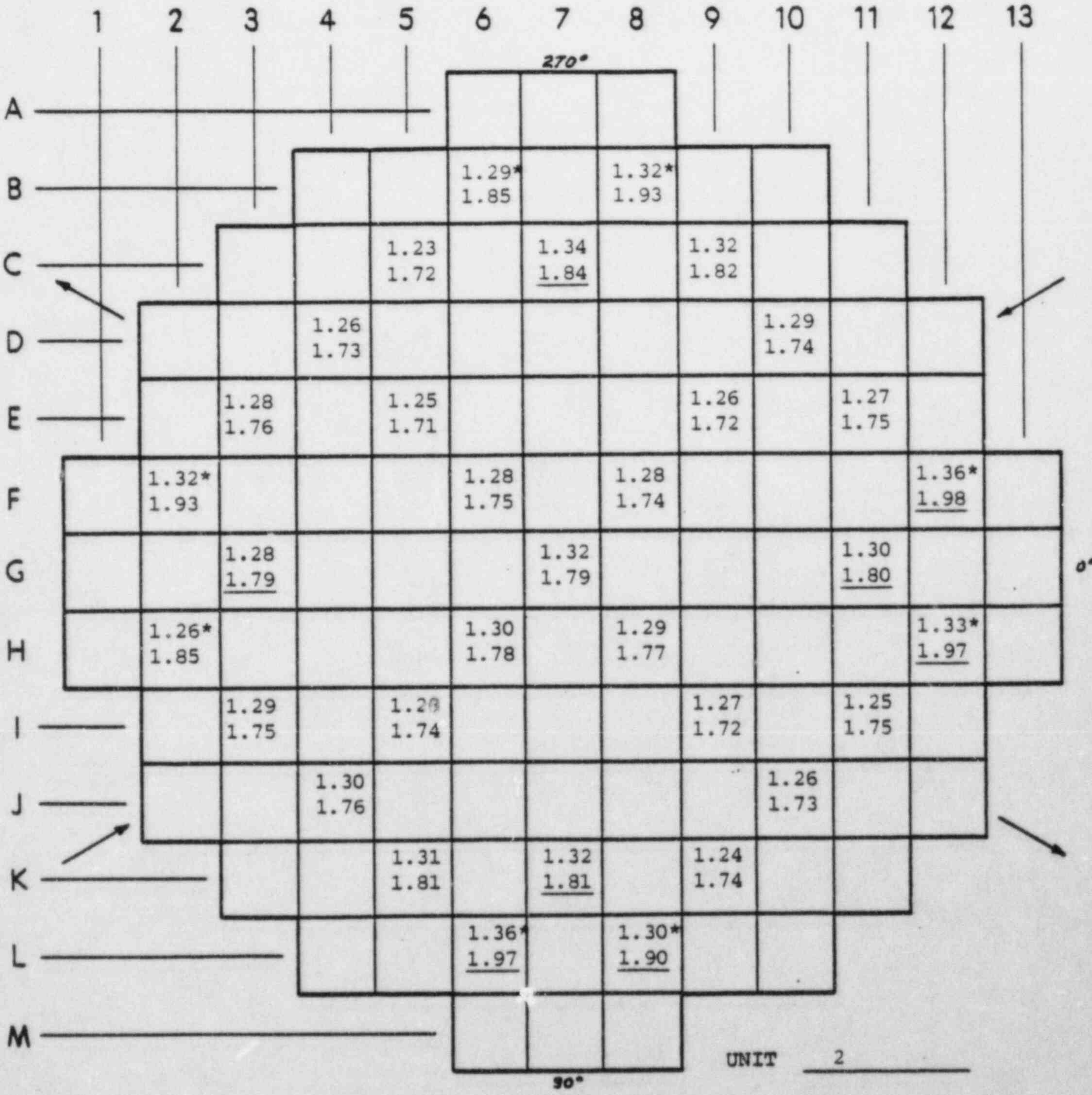

	1	2	3	4	5	6	7	8	9	10	11	12	13
A													
B						1.29* 1.85		1.32* 1.93					
C					1.23 1.72		1.34 1.84		1.32 1.82				
D				1.26 1.73						1.29 1.74			
E			1.28 1.76		1.25 1.71				1.26 1.72		1.27 1.75		
F		1.32* 1.93				1.28 1.75		1.28 1.74				1.36* 1.98	
G			1.28 1.79				1.32 1.79				1.30 1.80		
H		1.26* 1.85				1.30 1.78		1.29 1.77				1.33* 1.97	
I			1.29 1.75		1.28 1.74				1.27 1.72		1.25 1.75		
J				1.30 1.76						1.26 1.73			
K					1.31 1.81		1.32 1.81		1.24 1.74				
L						1.36* 1.97		1.30* 1.90					
M													

* ← Optimized Fuel Assembly
← TIME TO DASHPOT (SEC)
← TIME TO BOTTOM (SEC)
← New Control Rod

UNIT 2
DATE 11-17-84
TEMP. ∿ 535 °F
FLOW 100 %
PRESSURE ∿2000 psia

POINT BEACH NUCLEAR PLANT

CONTROL ROD TESTING
ROD DROP TIMES

RE-D6
(10-78)

Section 3.0 THERMOCOUPLE AND RTD CALIBRATION

During initial cycle heatup, thermocouple and loop RTD signals were recorded at different temperature levels under partial and full-flow conditions. See Table 3-1 for the results for full flow conditions. The RTD resistance readings were obtained at the protection racks in the control room using a digital multimeter that subtracted lead resistance. Thermocouple temperatures were read at the toggle readout panel.

Since the core was producing very little heat, the hot and cold leg RTD's were at about the same temperature. Thus both hot leg and cold leg readings were averaged into one temperature for the RTD's. The RTD resistances were converted to degrees Fahrenheit by using the vendor's calibration curves.

Due to the use of optimized fuel assemblies, the Improved Thermal Design Procedure (ITDP) was implemented. The ITDP has a requirement of 0.9% of span accuracy for the bypass manifold RTD's. To obtain the required accuracy, the existing Sostman RTD's were removed from the bypass manifolds for recalibration at PBNP. Because of poor calibration results, the Sostman RTD's were replaced with four Rosemount Model 176 and eight Model 189 RTD's.

It was found, however, that the yellow channel hot and cold leg RTD's being used were still not accurate enough as indicated in Table 3-1 and readings during initial power escalation. The spare RTD's (407A and 407B) were wired in place of 404A and 404B to obtain the required accuracy.

The T/C readout panel indicated that thermocouples at I-10, K-3, L-7, E-4, I-4, and M-6 were not functioning properly.

TABLE 3-1

RTD CALIBRATION CHECK

RTD Elements	RTD Temperatures from Measured Resistances (°F)				
Loop A - Cold Leg					
R 401B	413.11	466.76	475.10	515.39	539.25
R 405B	413.48	466.67	475.42	515.56	539.05
W 402B	413.56	467.11	475.61	515.90	539.77
Loop A - Hot Leg					
R 401A	412.81	466.02	474.63	514.80	538.38
R 405A	413.98	467.09	475.75	515.84	539.30
W 402A	413.37	466.88	475.27	515.50	538.96
Loop B - Cold Leg					
B 403B	414.23	467.77	476.30	516.62	539.99
B 407B	414.02	467.13	475.70	515.77	538.94
Y 404B	410.55	463.53	472.10	512.27	534.83
Loop B - Hot Leg					
B 403A	413.27	466.66	475.07	515.26	538.46
B 407A	414.43	468.66	476.22	516.62	539.15
Y 404A	414.70	468.56	476.88	517.42	540.57
RTD Average	413	467	475	516	539
T/C Average	421	479	--	524	545
Saturation Temp.	414	455	--	520	535

Section 4.0 PRESSURIZER TESTS

Section 4.1 Heater Capacity

Pressurizer heater capacity was calculated using volt and ampere readings for each group of heaters. Table 4-1 shows that heater capacity is above Technical Specification requirements of 100 KW minimum total.

TABLE 4-1

HEATER GROUP ENERGY INPUT

Group	I-Current (amps)	V-Voltage (volts)	KW-Energy Input $KW = \sqrt{3} \times V \times I/1000$
A	271	480	225
B	227	480	189
C	226	480	188
D	209	480	174
E	225	480	187
		TOTAL	963

Section 4.2 Spray Valve Effectiveness

Spray valve effectiveness is determined by measuring how fast each spray valve decreases pressurizer pressure when fully opened with the other valve closed and heaters off. For the test, spray valve "A" decreased pressure at the rate of 116 psi/min. Spray valve "B" decreased pressure at the rate of 113 psi/min. These are typical values and indicate that mass/flow through each valve is greater than design. It can be shown that given normal heat balance characteristics of the pressurizer, 200 gpm design spray flow decreases pressure by about 70 psi/min well below the results achieved above.

Section 4.3 Heater Effectiveness

Heater effectiveness is determined by measuring how fast pressurizer pressure increases with all heaters on and spray flow only through the bypass valves. For the test, pressurizer pressure increased at an average rate of 15.6 psi/min between 1840 and 2150 psia using all heaters. This is well above design heater capacity of 14.0 psi/min.

Section 5.0 REACTOR COOLANT SYSTEM

Section 5.1 RTD Manifold Flow

After the initial cycle heatup, the reactor coolant bypass flow through the RTD manifold was checked and found to be adequate for both loops. The flows were 215 gpm through Loop "A" and 190 gpm through Loop "B".

Section 5.2 Flow Transient Times

Table 5-1 gives the times to reach certain percentages of full-flow from the time a reactor coolant pump is tripped or started. The times are consistent with those obtained in previous measurements.

TABLE 5-1

REACTOR COOLANT FLOW TRANSIENT TIMES

Condition	Time to Reach 90% Flow (Sec.)	Time to Reach 50% Flow (Sec.)	Flow Through Active Loop (%)	Flow Through Inactive Loop (%)
A Tripped	2.1	14.0	----	0
B Tripped	2.1	14.5	----	0
A Not Running	----	----	----	-13.8
B Started	17.5*	----	>108.3(1)	----
A Started	18.0*	----	100	----
B Running	----	----	100	----
A Running	----	----	>107.9(1)	----
B Tripped	1.8	11.12	----	-17.3
A Running	----	----	100	----
B Started	19.6*	----	100	----
A Tripped	1.8	10.6	----	-14.3
B Running	----	----	107.7	----

* Time to reach 100% flow.

(1) Signal was off-scale high. Values given are for the highest scale reading.

Section 6.0 CONTROL SYSTEMS

There were no difficulties encountered during heatup or testing in the control systems of pressurizer level, pressurizer pressure, or the rod control system.

Section 7.0 TRANSIENTS

There were no significant transients during the startup or approach to full power. There were no violations of the fuel conditioning restrictions on power and rod stepping change rates.

Section 8.0 INITIAL CRITICALITY AND REACTIVITY COMPUTER CHECKS

Section 8.1 Initial Criticality

The approach to criticality was made in two phases. The first step, which began at 2020 hours on November 17, 1984, was the normal withdrawal of control rods until Bank D reached 180 steps at 2111 hours. Then the reactor coolant boron concentration was decreased by dilution until criticality was achieved. The dilution began at 2114 hours. The initial boron concentration was 1978 ppm. 10,400 gallons of water were used to reduce boron concentration by 594 ppm until criticality was achieved.

ICRR plots were maintained during each phase of the approach to criticality.

The reactor conditions at the time of criticality were determined to be as follows:

Date	November 18, 1984
Time	0100 hours
RCS Temperature	530°F
RCS Pressure	1985 psig
Rod Position	Bank D at 180 steps
Boron Concentration	1384 ppm

Section 8.2 Reactivity Computer Checks

1. Following criticality, acceptable zero power physics testing flux levels were determined. The flux level at which nuclear heat appeared was at 5×10^{-6} amps on N-35, 6×10^{-6} on N-36 and 3×10^{-6} amps on the Keithley picoammeter. Normal flux levels for physics testing are one-third of these values.

2. A check of the reactivity computer was made by comparing the computer's calculated reactivity for a certain doubling time versus the reactivity obtained from Figure A.1 of the WCAP. Reactor coolant system temperature was near 535°F. Table 8-1 shows the results of this check.

TABLE 8-1

REACTIVITY COMPUTER CHECKOUT

Bank D Steps		Measured Doubling Time (Sec.)	Measured Reactivity (pcm)	Calculated Reactivity (pcm)
From	To			
173	185	75.89	48	48
172	187	57.04	59	60
172	194	40.33	78	78

Section 9.0 CONTROL ROD WORTH MEASUREMENT

Section 9.1 Test Description

The rod worth verification utilizing rod exchange ("rod swap") was divided into two parts. In the first part, the reactivity worth of the reference bank was obtained from reactivity computer measurements and boron endpoint data during RCS boron dilution. In the second part, the critical height of the reference bank was measured after exchange with each remaining bank.

In the rod exchange technique, the reference bank is defined as that bank which has the highest worth of all banks, control or shutdown, when inserted into the core alone. For Cycle 11 the reference bank was Control Bank A (CA) as was the case in all prior rod swap tests.

Using the analog reactivity computer, reactivity measurements were made during the insertion of Control Bank A from the fully-withdrawn to the fully-inserted position. The average current (flux level) during the measurement was approximately 5 x 10^{-7} amps. Critical boron concentration measurements (boron endpoints) were made before and after the insertion of Control Bank A (see Section 11.0). Figure 9-1 shows the results of the differential worth measurements.

Starting at a critical position with the reference bank fully inserted and Control Bank C at 212 steps, a new critical configuration at constant RCS boron concentration was established with Control Bank C fully inserted and Control Bank A at 141 steps. Control Bank C was then withdrawn and Control Bank A inserted to one step to establish the initial conditions for the next exchange. This sequence was repeated until a critical position was established for the reference bank with each of the other banks individually inserted. Criticality determinations before and after each exchange were made with the reactivity computer.

The sequence of events during the rod exchange and a summary of the rod exchange data is presented in Table 9-1.

Section 9.2 Data Analysis and Test Results

The integral reactivity worth of the measured bank is inferred from the swapped portion of Control Bank A by the following equation:

$W_X^I = W_R^M - \Delta\rho_1 - (\alpha_X)\ (\Delta\rho_2) + W_X^E$ where:

W_X^I = The inferred worth of Bank X, pcm

W_R^M = The measured worth of the reference bank, Control A, from fully withdrawn to fully inserted with no other bank in the core.

α_X = A design correction factor taking into account the fact that the presence of another control rod bank is affecting the worth of the reference bank.

$\Delta\rho_2$ = The measured worth of the reference bank from the elevation at which the reactor is just critical with Bank X in the core to the reference bank fully withdrawn condition. This worth was measured with no other bank in the core.

$\Delta\rho_1$ = The measured worth of the reference bank from the fully inserted condition to the elevation at which the reactor was just critical prior to the worth measurement of Bank X. In this test $\Delta\rho_1$ is zero.

W_X^E = The worth of Bank X from the initial position (before the start of the exchange) to 228 steps. This worth is measured by the normal endpoint worth method.

Final values for the integral worth of control and shutdown banks inferred from the measurement data are tabulated in Table 9-2. Values for α_x were obtained from the design predictions are also listed in Table 9-2.

Section 9.3 Evaluation of Test Results

A comparison of the measured/inferred bank worths with design predictions is presented in Table 9-2.

In evaluating the test results, the standard review and acceptance criteria were used.

Review Criteria

a. The measured worth of the reference bank agrees with design predictions within ±10%.

b. The inferred individual worth of each remaining bank agrees with design predictions within ±15% or ±100 pcm whichever is greater.

c. The sum of the measured and inferred worths of all control and shutdown banks is less than 1.1 times the predicted sum.

Acceptance Criteria

a. The sum of the measured/inferred worths of all control and shutdown banks is greater than 0.9 times the predicted sum.

As shown on Table 9-2, all review and acceptance criteria were met.

FIGURE 9-1

CONTROL BANK A WORTH

PBNP UNIT 2 CYCLE 11
BOL HZP

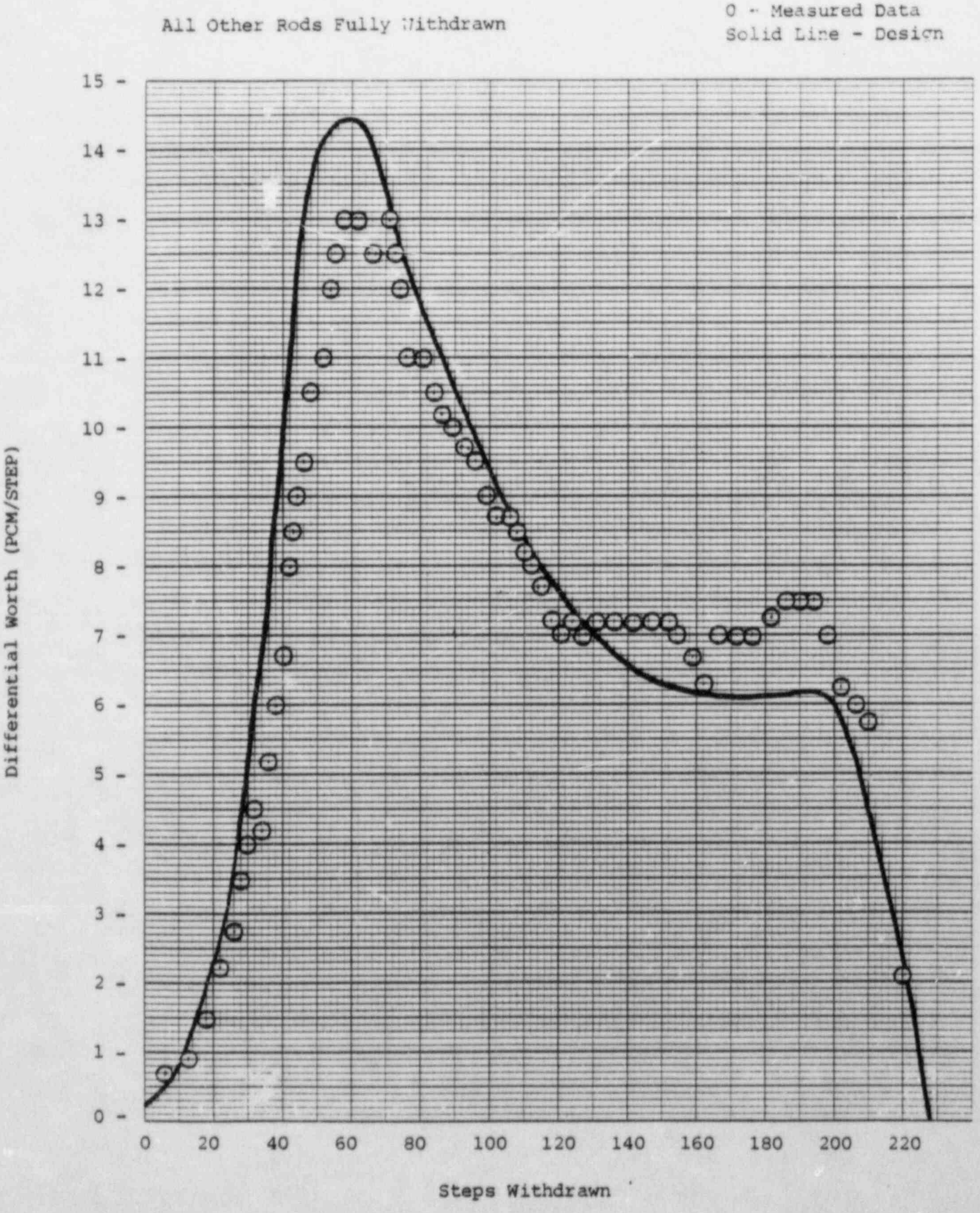

TABLE 9-1

CRITICAL ROD CONFIGURATION DATA
11-19-84

Bank Measured	Time	RCS Tavg (°F)	CA Position (Steps)	Measured Bank Position (Steps)
CC	1721	530	1	212
CC	1732	530	141	1
CC	1744	531	1	214
SB	1747	531	1	217
SB	1757	531	131	1
SB	1808	531	1	217
SA	1819	531	1	213
SA	1827	531	127	1
SA	1839	531	1	214
CD	1849	531	1	213
CD	1856	531	83	1
CD	1905	531	1	220
CB	1906	531	1	218
CB	1912	530	101	1
CB	1920	530	1	220

Boron concentration was 1190 ppm.

TABLE 9-2

COMPARISON OF INFERRED/MEASURED BANK WORTHS WITH DESIGN PREDICTIONS

Bank X	$\Delta\rho_2$ (pcm)	α_X	W_X^E (pcm)	W_X^I (pcm)	W_X^P (pcm)	$\left(\frac{I-P}{P}\right) \times 100$ (%)
CC	530	0.956	37	1125	1149	- 2.1
SB	602	1.009	23	1011	996	+ 1.5
SA	631	0.953	23	1017	993	+ 2.4
CD	1014	0.991	24	607	580	+ 5.9
CB	837	1.077	27	714	690	+ 3.7
CA	----	----	----	1595	1650	- 3.3
			TOTAL	6076	6058	+ 0.3

Section 10.0 TEMPERATURE COEFFICIENT MEASUREMENTS

Isothermal temperature coefficient measurements were taken during zero power physics testing. The measurement test conditions and results are given in Table 10-1. The measured values are the average of the recorded reactor coolant system heatups and cooldowns. Reactivity from the reactivity computer and reactor coolant system temperature were recorded on an X-Y plotter and two-pen recorder.

The measured temperature coefficients are within the review criteria of ±3 pcm/°F.

TABLE 10-1

ISOTHERMAL TEMPERATURE COEFFICIENTS

Control Bank Configuration	Boron Conc. ppm	Avg. Temp. °F	Measured pcm/°F	Design* pcm/°F	Difference pcm/°F (M-D)
ARO	1351	534	-3.1	-3.1	0.0
A in	1189	530	-7.3	-6.3	-1.0

*WCAP Figure 5.1 and Figure 5.8

Section 11.0 BORON WORTH AND ENDPOINT MEASUREMENTS

Figure 11-1 shows RCS boron concentration during zero power physics testing. Table 11-1 shows results of the endpoint measurements. Design values are for 530°F testing temperature. The measured boron worth was obtained by dividing bank worth (pcm) into change in boron concentration between the endpoints.

Review criterion was not met (±0.5 pcm/ppm). This is a typical problem with boron endpoint measurements where measured boron endpoints are not close to design.

TABLE 11-1

BORON WORTH AND ENDPOINTS

	Endpoint		Bank Worth		Boron Worth	
Bank Configuration	Design(1) (ppm)	Measured (ppm)	Design (pcm)	Measured (pcm)	Design(2) (pcm/ppm)	Measured (pcm/ppm)
ARO	1373	1355	---	---	-9.19	---
CA in	1189	1192	1650	1595	-9.15	-9.8

(1) Figure 5.1
Table A.2

(2) Figure 2 - Supplement to WCAP, Letter 84WE-G-080
Table A.2

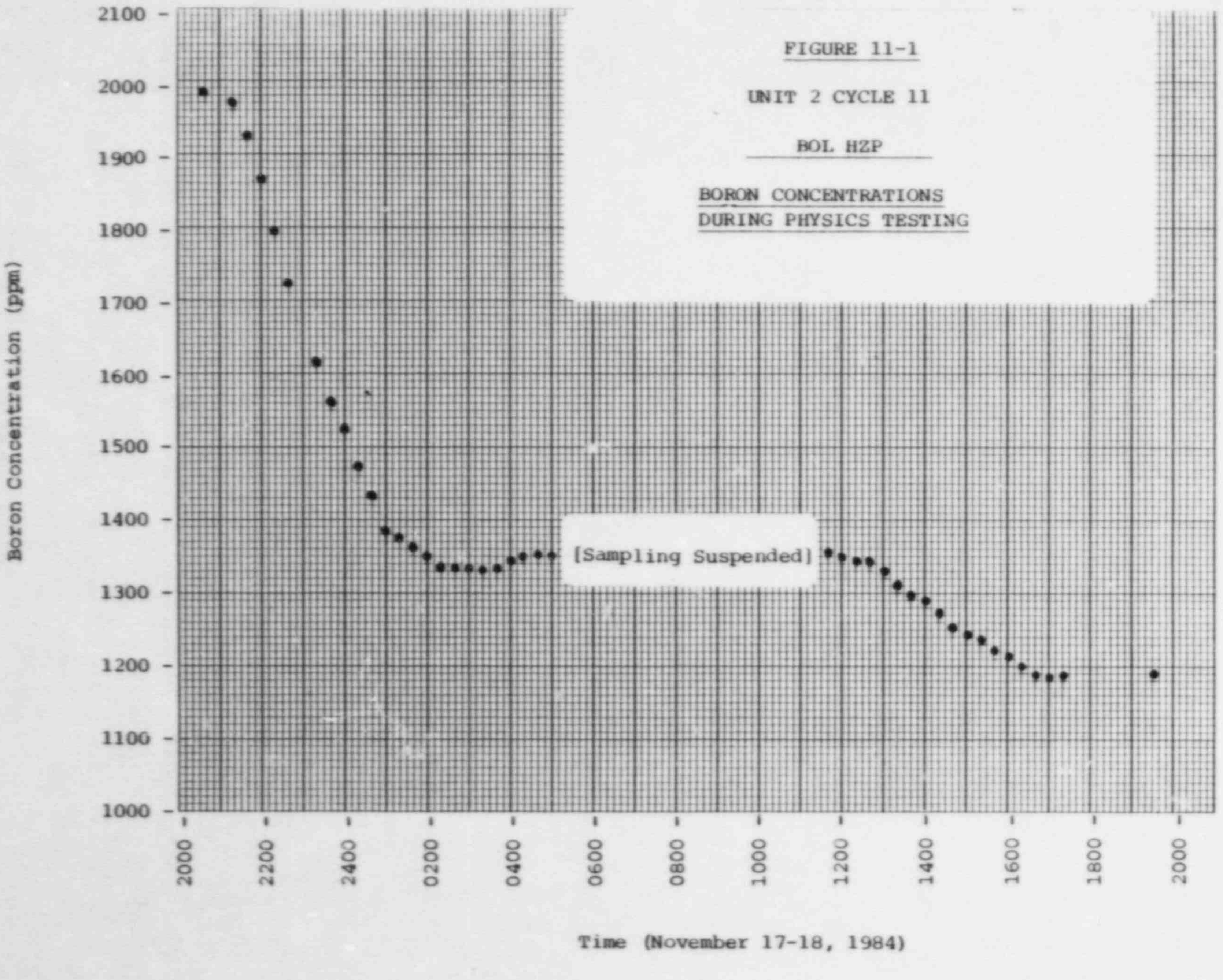

FIGURE 11-1

UNIT 2 CYCLE 11

BOL HZP

BORON CONCENTRATIONS
DURING PHYSICS TESTING

Section 12.0 POWER DISTRIBUTION

Table 12-1 illustrates the lowering of maximum hot channel factors during initial power increase to full load. More flux maps were required because allowed power levels based on maximum hot channel factors were less than 100% for the HZP flux map. Allowed power levels were calculated using the relationships for $F\Delta H$ and FQ versus power level in Technical Specification 15.3.10.B.1.a. The relationships have been changed due to the use of optimized fuel assemblies in Cycle 11. Zero power flux map results typically do not show that full power operation is permitted due to hot channel factor limitations.

Measured power sharing factors ($F\Delta H$) for each fuel assembly were compared to predicted values. Differences of more than 5% were listed in Figure 12-1 for the ARO HZP flux map and for a full power map (No. 9) taken after a month of operation.

Figures 12-2 and 12-3 show the actual power sharing factors at each location for the same flux maps.

Measured axial power distribution compared to design is shown in Figures 12-4 and 12-5 for the same flux maps.

TABLE 12-1

INITIAL POWER ESCALATION FLUX MAP RESULTS

Flux Map Number	Date	Power (%)	Thimbles Missing	Allowed Power (%)	
				FΔHN	FQN
1	11-18-84	0	5	100	76
2	11-20-84	20	1	112	104
3	11-26-84	50	1	117	113
* 4	11-27-84	50	2	114	109
* 5	11-27-84	50	1	116	107
6	12-03-84	100	1	116	118
* 7	12-04-84	100	1	116	115
* 8	12-04-84	100	1	116	115
9	12-19-84	100	1	117	119

* QAO flux maps taken when delta flux or control rods were not near their normal operating positions.

FIGURE 12-1

UNIT 2 CYCLE 11 STARTUP

$F^N_{\Delta H}$ DIFFERENCES GREATER THAN ±5%

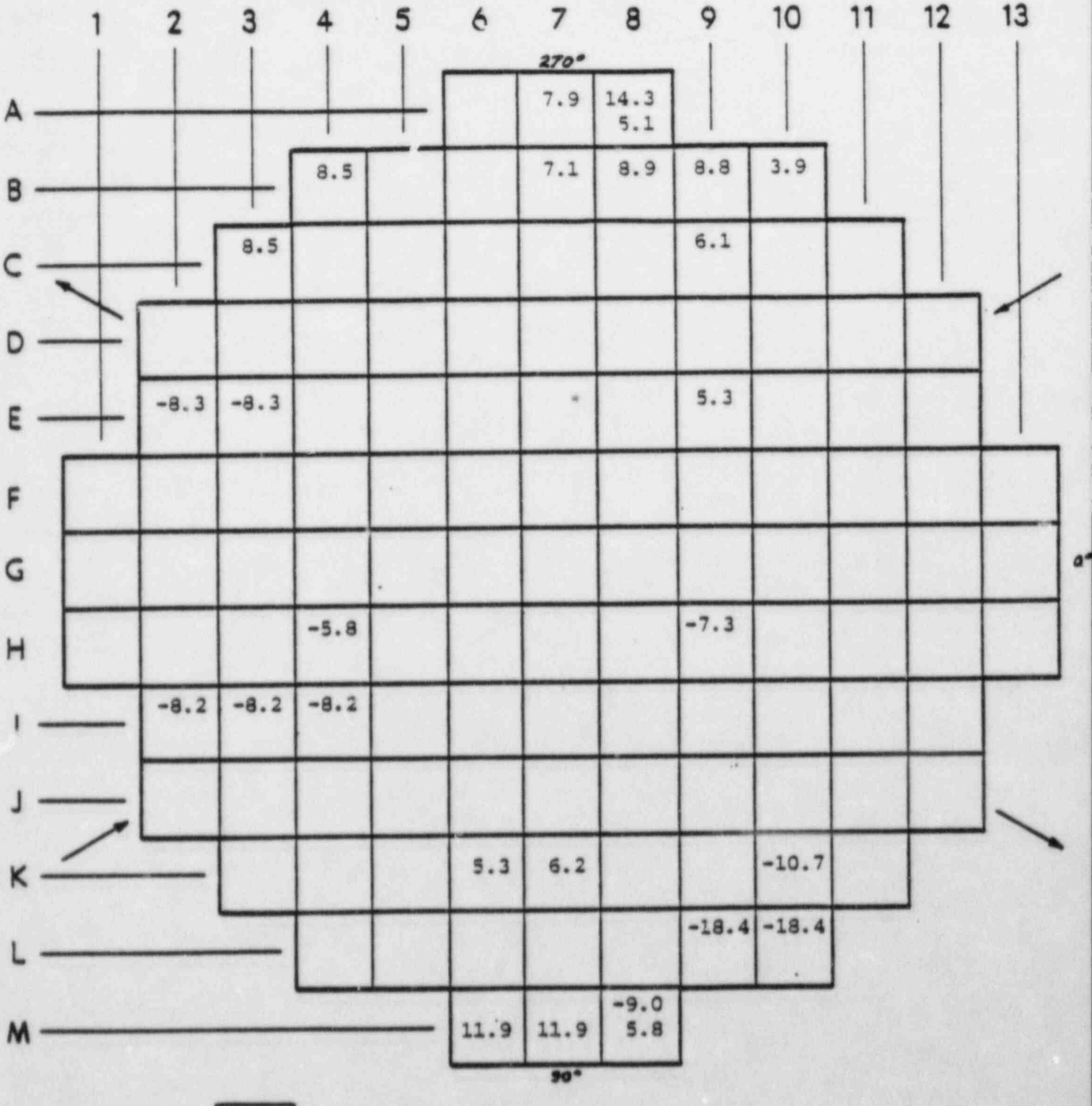

	1	2	3	4	5	6	7	8	9	10	11	12	13
A							7.9	14.3 5.1					
B				8.5			7.1	8.9	8.8	3.9			
C			8.5						6.1				
D													
E		-8.3	-8.3						5.3				
F													
G													
H				-5.8					-7.3				
I		-8.2	-8.2	-8.2									
J													
K						5.3	6.2			-10.7			
L									-18.4	-18.4			
M						11.9	11.9	-9.0 5.8					

☐ ← Flux Map #1 Difference (%) - HZP
← Flux Map #9 Difference (%) - Full Power

$$\% \text{ Diff.} = \frac{M-E}{E}$$

POINT BEACH NUCLEAR PLANT

FIGURE 12-2

POWER DISTRIBUTION, HZP, ARO

PBFM 211-1A HZP ARO 11/18/84

	1	2	3	4	5	6	7	8	9	10	11	12	13
A						0.309 0.313 1.2	0.284 0.307 7.9	0.312 0.357 14.3					
B				0.408 0.443 8.5	0.936 0.947 1.2	1.099 1.112 1.2	0.949 1.016 7.1	1.111 1.209 8.9	0.971 1.056 8.8	0.436 0.453 3.9			
C			0.470 0.510 8.5	1.083 1.122 3.6	1.153 1.151 -0.2	0.996 0.998 0.1	0.893 0.916 2.6	0.998 1.043 4.4	1.216 1.290 6.1	1.183 1.229 3.9	0.519 0.527 1.5		
D		0.403 0.403 -0.1	1.119 1.123 0.3	1.113 1.151 3.4	1.181 1.185 0.3	1.136 1.142 0.5	0.958 0.986 2.9	1.156 1.206 4.3	1.276 1.339 5.0	1.313 1.359 3.5	1.213 1.238 2.0	0.456 0.463 1.5	
E		0.905 0.830 -8.3	1.113 1.021 -8.3	1.165 1.150 -1.3	1.199 1.199 -0.0	1.219 1.222 0.3	1.244 1.290 3.7	1.251 1.307 4.5	1.294 1.363 5.3	1.311 1.345 2.6	1.284 1.317 2.6	1.036 1.063 2.6	
F	0.307 0.296 -3.7	1.074 1.034 -3.7	0.953 0.919 -3.6	1.107 1.083 -2.2	1.199 1.203 0.4	1.215 1.236 1.7	1.203 1.261 4.8	1.254 1.244 -0.8	1.285 1.282 -0.3	1.222 1.202 -1.6	1.086 1.120 3.1	1.205 1.252 3.9	0.340 0.354 4.1
G	0.315 0.317 0.7	0.956 0.924 -3.3	0.894 0.862. -3.6	0.954 0.915 -4.1	1.234 1.231 -0.2	1.201 1.219 1.5	0.883 0.906 2.6	1.235 1.205 -2.4	1.293 1.244 -3.8	1.016 0.969 -4.7	0.963 0.954 -1.0	1.029 1.069 3.9	0.316 0.329 4.1
H	0.321 0.324 0.7	1.144 1.101 -3.7	1.035 0.994 -3.9	1.174 1.106 -5.8	1.252 1.254 0.1	1.249 1.275 2.0	1.241 1.240 -0.1	1.283 1.220 -4.9	1.290 1.197 -7.3	1.214 1.159 -4.5	1.058 1.035 -2.1	1.186 1.202 1.4	0.336 0.350 4.1
I		0.994 0.913 -8.2	1.237 1.136 -8.2	1.280 1.175 -8.2	1.281 1.286 0.4	1.260 1.265 0.4	1.295 1.309 1.1	1.310 1.325 1.2	1.327 1.305 -1.7	1.325 1.266 -4.4	1.273 1.217 -4.4	1.023 0.987 -3.5	
J		0.442 0.460 4.2	1.186 1.236 4.2	1.297 1.352 4.2	1.278 1.332 4.2	1.181 1.214 2.8	1.006 1.050 4.3	1.229 1.284 4.5	1.328 1.354 1.9	1.345 1.299 -3.4	1.226 1.184 -3.4	0.455 0.439 -3.5	
K			0.513 0.525 2.4	1.181 1.210 2.5	1.230 1.260 2.4	1.029 1.083 5.3	0.942 1.000 6.2	1.077 1.058 -1.7	1.283 1.218 -5.1	1.228 1.097 -10.7	0.533 0.51 -3.3		
L				0.439 0.449 2.3	0.990 1.013 2.3	1.150 1.179 2.6	1.002 1.028 2.6	1.187 1.131 -4.7	1.031 0.841 -18.4	0.458 0.374 -18.4			
M						0.325 0.324 -0.1	0.300 0.300 -0.1	0.333 0.303 -9.0					

PBFM 211-1A HZP ARO 11/18/84

0.000 PREDICTED FDHN
0.000 MEASURED FDHN
0.0 % DIFF. (M-P)/P

0.0 % FZ = 1.685 FDHN = 1.520 AT F12DE FQ = 2.545 AT F12DE

FIGURE 12-3

POWER DISTRIBUTION AT POWER

```
                       PBFM 211-9  1500.9 MWT  ROUTINE  12/19/84

          1       2       3       4       5       6       7       8       9      10      11      12      13

                                              0.356   0.334   0.355
 A                                            0.354   0.343   0.373
                                               -0.3     2.4     5.1

                              0.453   0.984   1.149   1.006   1.144   0.990   0.462
 B                            0.463   0.980   1.145   1.030   1.185   1.026   0.472
                                2.1    -0.3    -0.3     2.4     3.6     3.6     2.0

                      0.517   1.125   1.183   1.041   0.937   1.026   1.201   1.164   0.537
 C                    0.528   1.138   1.182   1.045   0.947   1.050   1.235   1.186   0.542
                        2.1     1.2    -0.0     0.4     1.1     2.3     2.8     2.0     0.9

              0.448   1.160   1.142   1.201   1.166   0.991   1.164   1.241   1.258   1.178   0.473
 D            0.454   1.176   1.155   1.198   1.168   1.001   1.191   1.262   1.270   1.180   0.478
                1.3     1.4     1.2    -0.3     0.2     1.0     2.3     1.7     1.0     0.1     0.9

              0.956   1.147   1.188   1.209   1.219   1.233   1.227   1.251   1.258   1.235   1.021
 E            0.962   1.154   1.190   1.207   1.220   1.234   1.233   1.245   1.249   1.218   1.000
                0.6     0.6     0.2    -0.2     0.1     0.1     0.5    -0.5    -0.7    -1.4    -2.1

      0.350   1.125   1.002   1.142   1.203   1.207   1.189   1.221   1.241   1.197   1.072   1.186   0.369
 F    0.355   1.140   1.010   1.142   1.203   1.207   1.189   1.216   1.235   1.182   1.053   1.166   0.364
        1.4     1.4     0.8    -0.1    -0.0     0.0    -0.1    -0.4    -0.5    -1.3    -1.8    -1.7    -1.3

      0.360   1.006   0.937   0.988   1.228   1.189   0.897   1.201   1.247   1.011   0.963   1.035   0.352
 G    0.362   1.004   0.935   0.981   1.230   1.195   0.894   1.191   1.232   0.992   0.941   1.017   0.347
        0.7    -0.1    -0.2    -0.7     0.2     0.5    -0.3    -0.9    -1.2    -1.8    -2.3    -1.7    -1.3

      0.361   1.168   1.056   1.181   1.230   1.221   1.208   1.234   1.237   1.184   1.045   1.169   0.365
 H    0.363   1.165   1.054   1.168   1.234   1.227   1.204   1.224   1.217   1.166   1.026   1.154   0.363
        0.6    -0.2    -0.2    -1.1     0.3     0.5    -0.3    -0.8    -1.6    -1.6    -1.8    -1.2    -0.6

              1.008   1.219   1.248   1.246   1.227   1.251   1.253   1.259   1.256   1.217   1.006
 I            0.993   1.197   1.226   1.248   1.229   1.242   1.243   1.240   1.238   1.198   0.991
               -1.4    -1.8    -1.8     0.2     0.2    -0.7    -0.8    -1.5    -1.4    -1.6    -1.5

              0.468   1.169   1.252   1.241   1.171   1.006   1.198   1.259   1.264   1.175   0.469
 J            0.460   1.156   1.239   1.235   1.159   0.997   1.187   1.246   1.251   1.158   0.461
               -1.7    -1.1    -1.1    -0.5    -1.0    -0.9    -0.9    -1.0    -1.0    -1.4    -1.6

                      0.535   1.162   1.204   1.034   0.951   1.063   1.226   1.176   0.540
 K                    0.528   1.148   1.192   1.011   0.936   1.051   1.215   1.165   0.530
                       -1.2    -1.2    -1.0    -2.2    -1.6    -1.1    -0.9    -1.0    -1.8

                              0.463   0.994   1.153   1.019   1.172   1.012   0.471
 L                            0.458   0.984   1.210   1.069   1.208   1.006   0.468
                               -1.0    -1.0     4.9     4.9     3.0    -0.6    -0.6

                                              0.358   0.339   0.363
 M                                            0.401   0.379   0.384
                                               11.9    11.9     5.8

                       PBFM 211-9  1500.9 MWT  ROUTINE  12/19/84


          CONTROL ROD POSITIONS (STEPS)                                 0.000  PREDICTED FDHN
 SHDWN  SHDWN  CNTRL  CNTRL  CNTRL  CNTRL                               0.000  MEASURED FDHN
   A      B      A      B      C      D                                   0.0  % DIFF. (M-P)/P
 225.   225.   228.   228.   228.   213.

 POWER 1501. MWT  98.8 %     FZ = 1.161   FDHN = 1.443 AT  L 8JD   FQ = 1.698 AT  L 8JD
```

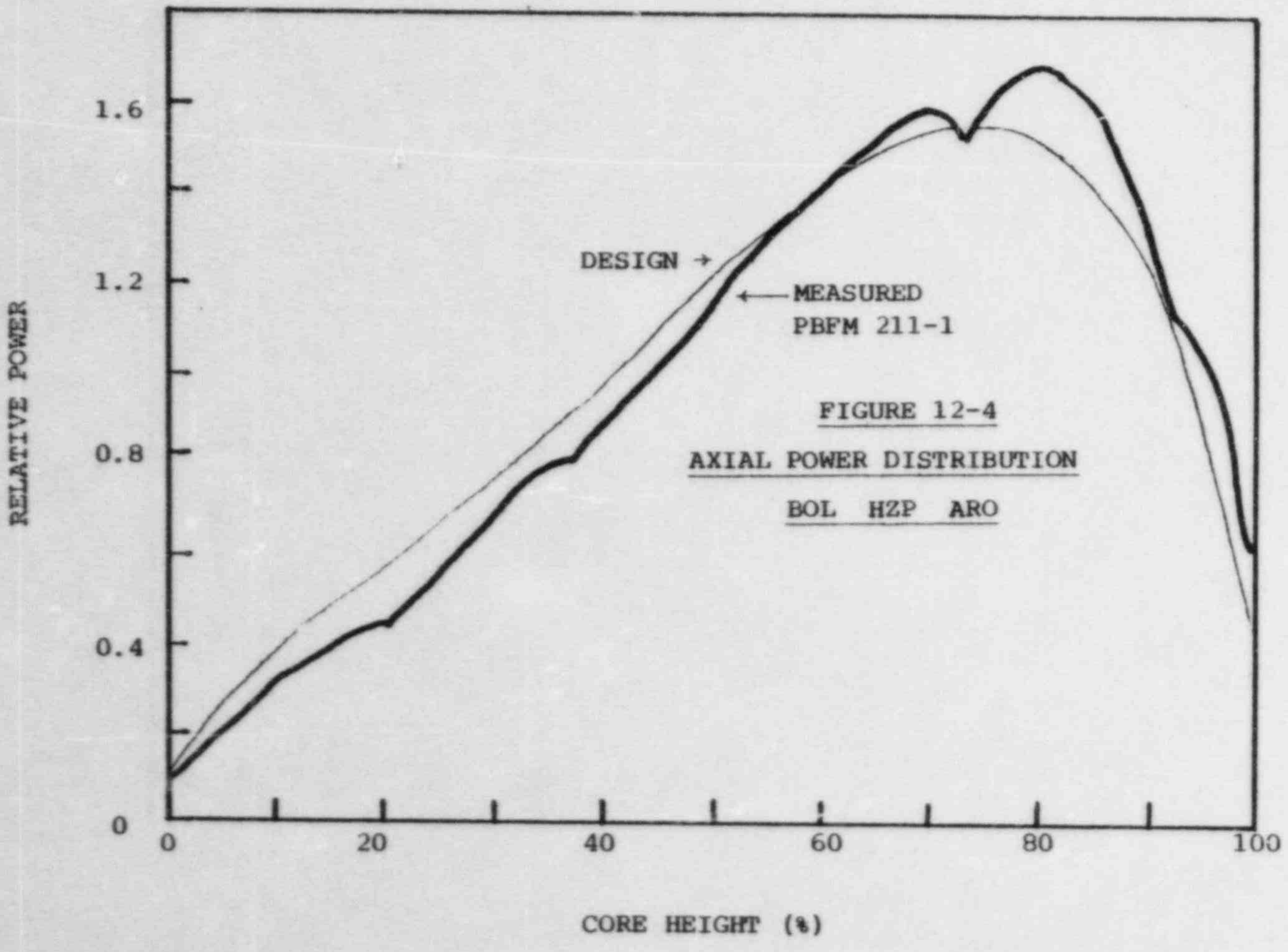

FIGURE 12-4

AXIAL POWER DISTRIBUTION

BOL HZP ARO

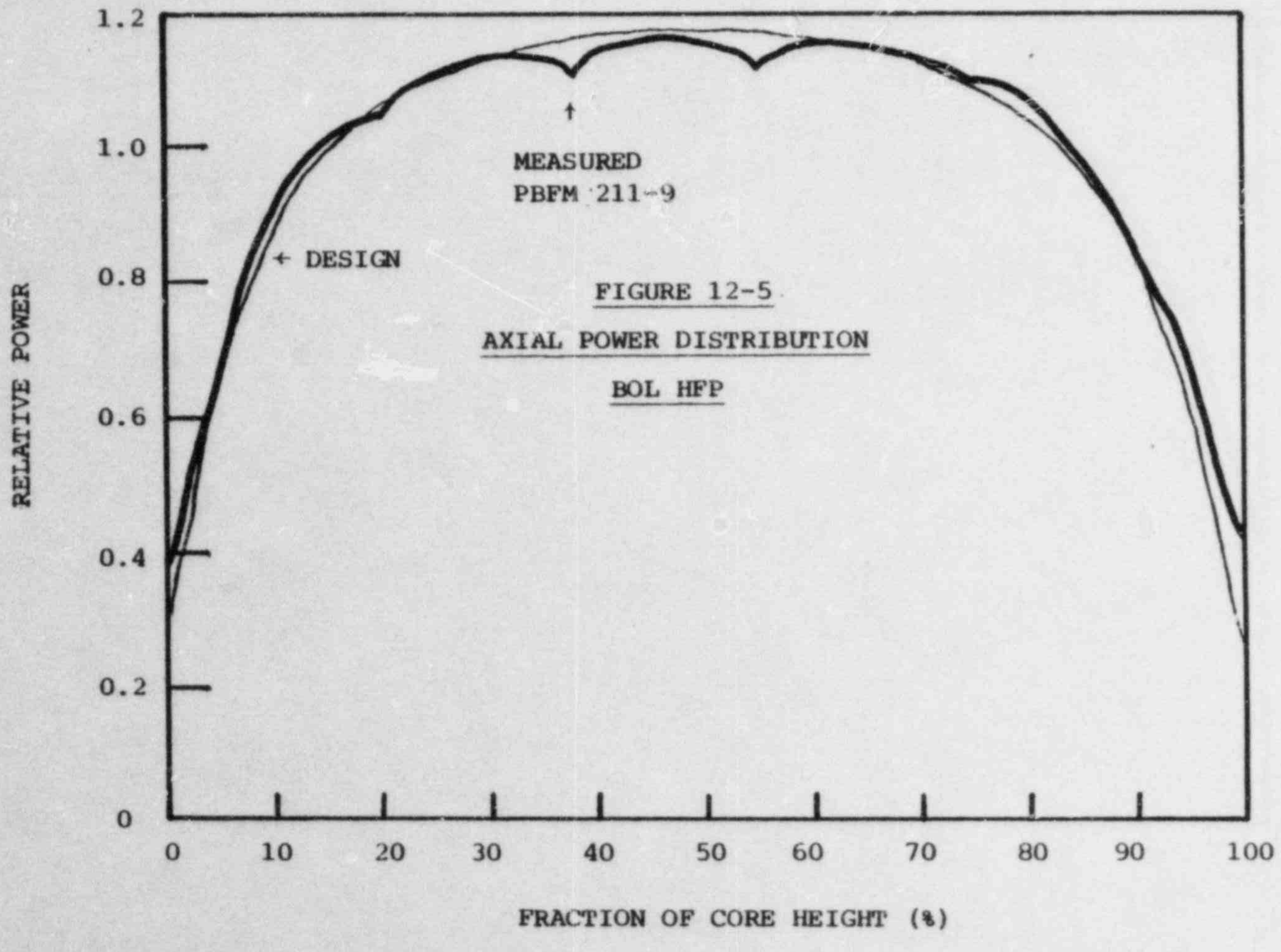

FIGURE 12-5

AXIAL POWER DISTRIBUTION

BOL HFP

Section 13.0 XENON REACTIVITY

Xenon reactivity behavior data for Unit 2 Cycle 11 was supplied by Westinghouse as part of the WATCH data package. Point Beach code XENALG will be run with a TDF1 of 0.95 and a TDF2 of 1.2 to remain consistent with the Xenon Tables. Tables are supplied for BOL, MOL and EOL conditions.

Section 14.0 SHUTDOWN MARGIN CONSIDERATIONS

Rod swap results were within acceptance criteria and were accepted as valid proof of rod worth for shutdown margin determination. See Section 9.0 for rod swap details. Thus WCAP Table 6.3 was accepted as a valid shutdown margin determination. Table 14-1 calculates the excess worth available to Unit 2 Cycle 11.

TABLE 14-1

EXCESS SHUTDOWN WORTH AVAILABLE FOR A FULL POWER TRIP

	BOL (pcm)	EOL (pcm)
Shutdown Margin From WCAP Table 6.3	-4230	-3500
- Required Shutdown	-1000	-2770
= Excess Worth	-3230	- 730

Section 15.0 EXCORE DETECTOR BEHAVIOR

Section 15.1 Excore Detector Current Versus Power Level

The upper and lower excore detector currents for each power range channel were recorded and calorimetrics were performed at various power levels. The upper and lower detector currents were summed for each channel and then normalized to obtain predicted currents for 100% power. These 100% currents are listed in Table 15-1.

Intermediate range detector currents versus power level are shown in Figure 15-1. The intermediate range detector trip signals activated at about 2.9 x 10^{-4} amps and 3.2 x 10^{4} amps for N35 and N36 respectively. From Figure 15-1, the trip signals occurred between 28% and 30% power as expected.

FIGURE 15-1

INTERMEDIATE RANGE DETECTOR RESPONSE TO POWER LEVEL

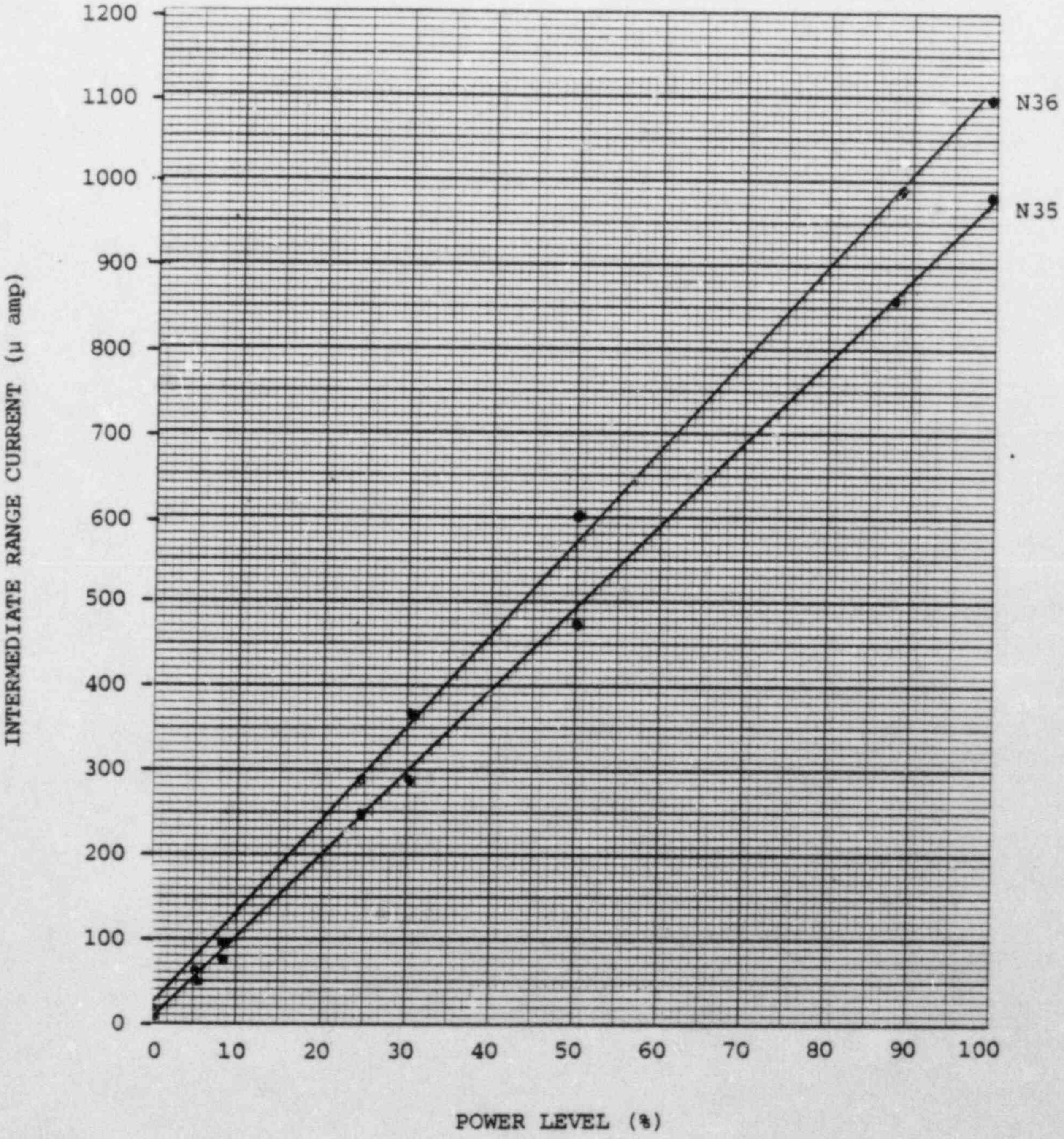

TABLE 15-1

100% CURRENTS (μ AMPS)

	41	42	43	44
Cycle 11	576	626	379	573
Cycle 10	625	641	403	574
Cycle 9	615	651	415	610

Section 15.2 Excore Axial Offset Response

Excore axial offset responds to actual incore axial offset (calculated from flux map data) in a linear fashion but not with a one-to-one correspondence. Excore axial offset "sees" only about 70% of the actual axial offset. Table 15-2 shows the historic response of the detectors.

Section 15.3 Channel Calibration

The currents measured during flux maps at three different axial offsets were first corrected for quadrant tilt by dividing each channel current by the quadrant tilt factor calculated by PBCORE for the associated quadrant. Then because each flux map was taken at a slightly different power level, the currents from two maps were ratioed up or down by the percent the power level had changed from the reference map.

Straight line fits of the "corrected" currents for each channel versus incore axial offset as determined by the flux maps were obtained. The intersection of the line with zero axial offset was the calibration current at the power level of the reference map.

Power range quadrant tilt alarms were meant for rapidly developing tilts. Natural core tilts were washed out to prevent a bias in alarming of rapidly occurring tilts. This was accomplished by multiplying the calibration currents for each channel by the quadrant tilt factors calculated by PBCORE, to obtain "tilt free" calibration currents. Thus, after the "tilt free" calibration currents were entered, the computer and the Hagan recorders indicated the same power (voltage) on all upper half quadrants and the same power on all lower half quadrants.

In actual practice, the "tilt free" calibration currents are ratioed to a power level slightly above normal operating full power to make it possible for the currents to be set in at power. Table 15-3 lists the actual "tilt free" calibration currents at 100% power at BOL.

TABLE 15-2

EXCORE AXIAL OFFSET RESPONSE HISTORY

	Slope (Incore vs. Excore)			
	41	42	43	44
Cycle 11	1.45	1.37	1.17	1.38
Cycle 10	1.56	1.55	1.27	1.50
Cycle 9	1.49	1.58	1.27	1.66

TABLE 15-3

BOL CALIBRATION CURRENTS (100%)

	41	42	43	44
T	304	321	201	290
B	265	291	168	271

Section 16.0 OVERPOWER, OVERTEMPERATURE AND DELTA FLUX SETPOINTS CALCULATION

Section 16.1 Overpower and Overtemperature ΔT Setpoints Calculation

Discussion of the setpoints and equations has been sufficiently covered in previous reports.

The equations are:

$$\text{Overpower } \Delta T \left(\frac{1}{1+\tau_3 S} \right)$$

$$\leqq \Delta T_\circ \left[K_4 - K_5\left(\frac{\tau_5 S}{\tau_5 S + 1}\right)\left(\frac{1}{1+\tau_4 S} \right) T - K_6 \left[T\left(\frac{1}{1+\tau_4 S} \right) - T'\right] - f(\Delta I)\right]$$

$$\text{Overtemperature } \Delta T\left(\frac{1}{1+\tau_3 S} \right)$$

$$\leqq \Delta T_\circ \left(K_1 - K_2\left(T\left(\frac{1}{1+\tau_4 S} \right) - T^1\right)\left(\frac{1+\tau_1 S}{1+\tau_2 S} \right) + K_3 (P-P^1) - f(\Delta I)\right)$$

See Tables 16-1 and 16-2 for the constants associated with this cycle of operation.

Section 16.2 Delta Flux Setpoints Calculation

The overpower and overtemperature ΔT setpoints are reduced when the excore detectors sense a power mismatch between the top and bottom of the core. The dead band is +5% and -17% before the setpoints are reduced. For each percent (more than 5%) the top detector output exceeds the bottom detector, the setpoints are reduced an equivalent of 2% of the rated power. For each percent (more than -17%) the bottom detector exceeds the top detector, the setpoints are reduced an equivalent of 2% of rated power.

TABLE 16-1

OVERTEMPERATURE ΔT CONSTANTS

ΔT_o = Indicated ΔT at rated power, °F

T = Average temperature, °F

T^1 = 574.2°F

P = Pressurizer pressure, psig

P^1 = 2235 psig

K_1 ≦1.117 for operation at 2250 psia primary system pressure

≦1.30 for operation at 2000 psia primary system pressure

K_2 = 0.0150

K_3 = 0.000791

$\tau 1$ = 25 seconds

$\tau 2$ = 3 seconds

$\tau 3$ = 2 seconds for Rosemount or equivalent RTD

= 0 seconds for Sostman or equivalent RTD

$\tau 4$ = 2 seconds for Rosemount or equivalent RTD

= 0 seconds for Sostman or equivalent RTD

TABLE 16-2

OVERPOWER ΔT CONSTANTS

ΔT_o = Indicated ΔT at rated power, °F

T = Average temperature, °F

$T' = 574.2°F$

$K_4 \leqq 1.089$ of rated power

$K_5 = 0.0262$ for increasing T

$= 0.0$ for decreasing T

$K_6 = 0.00123$ for $T \geqq T$

$= 0.0$ for $T < T'$

$\tau5$ = 10 seconds

$f(\Delta I)$ as defined in Section 16.2

$\tau3$ = 2 seconds for Rosemount or equivalent RTD

= 0 seconds for Sostman or equivalent RTD

$\tau4$ = 2 seconds for Rosemount or equivalent RTD

= 0 seconds for Sostman or equivalent RTD

Section 17.0 FUEL PERFORMANCE

Reactor coolant activity is summarized in Table 17-1 and indicates good fuel integrity.

Because of low Cycle 10 activity, no fuel assembly failures were expected. Thus, there were no fuel assembly inspections scheduled other than the demonstration optimized fuel assemblies. Those assemblies were in good condition.

TABLE 17-1

TYPICAL ISOTOPIC COMPOSITION OF PRIMARY COOLANT ACTIVITY

Isotope	Half Life	End of Cycle 10 μC/cc x 10^{-1}	Start of Cycle 11 μC/cc x 10^{-1}
I-131	8.05 days	0.1	0.0
I-132	2.3 hours	1.5	0.7
I-133	21 hours	1.0	0.5
I-134	53 minutes	2.6	1.2
I-135	6.7 hours	2.0	1.0
	TOTAL	7.1	3.5
Gross Activity (μCi/cc) 30 minute decay		0.6	0.3

Section 18.0 CONCLUSION

The use of optimized fuel assemblies produced no unusual physics testing results. The use of optimized fuel assemblies had no significant effects on other phases of startup testing.